Shift of C3 deposition from localization in the glomerulus into the tubulo-interstitial compartment in the absence of secreted IgM in immune complex glomerulonephritis

C. Vaculik,* B. M. Rüger,*
G. Yanagida,* D. Hollemann,*
A. Soleiman,† U. M. Losert,‡ J. Chen§
and M. B. Fischer*

*Department of Transfusion Medicine, †Clinical
Institute of Pathology, ‡Core Unit for Biomedical
Research, Medical University of Vienna, Vienna,
Austria, and §Department of Biochemistry,
Cancer Center MIT, Boston, MA, USA

Summary

The role of secretory IgM in protecting kidney tissue from immune complex glomerulonephritis induced by 4 mg horse spleen apoferritin and 0·05 mg lipopolysaccharide has been investigated in mutant mice in which B cells do not secrete IgM, but are capable of expressing surface IgM and IgD and secreting other Ig isotypes. Glomerular size, number of glomeruli per cross-section, glomerular cellularity and urine content of protein and creatinine was comparable in treated secreted IgM (sIgM)-deficient and wild-type mice. Assessment of urinary proteins by sodium dodecyl sulphate-polyacrylamide gel electrophoresis showed a 30 kDa low molecular weight protein in treated sIgM-deficient animals only, reflecting dysfunction of proximal tubules. A shift of bound C3 from glomeruli to the tubulo-interstitial compartment in sIgM-deficient mice also suggests tubulo-interstitial damage. In contrast, local C3 synthesis within the kidney tissue did not differ between the two treated groups. Apoptosis physiologically present to maintain kidney cell homeostasis was increased slightly in treated wild-type mice. These results indicate that secretory IgM can protect the tubulo-interstitial compartment from immune complex-induced damage without having an effect on the glomerulus.

Keywords: complement C3, immune complex glomerulonephritis, LPS, secretory IgM

Introduction

The innate immune system employs a number of soluble proteins and cell-surface receptors that provide a first line of defence against microbial infection, and in addition has an instructive role on the acquired immune response [1]. Therefore, different components of the innate immune system can play a harmful as well as a beneficial role in renal disease. The formation of immune complexes comprising antigen, antibodies and complement proteins contributes to the clearance of antigen from the circulation, which prevents antigen spreading and subsequent damage of the kidney [2,3]. Immune complex (IC) formation and deposition is associated with a variety of immune-mediated renal diseases, such as membranoproliferative glomerulonephritis (GN), IgA nephropathy and lupus nephritis, but was also found in ischaemia reperfusion injury and during allograft rejection response of kidney transplants [4–11]. In different renal diseases the localization of ICs in the kidney, either by deposition of circulating ICs or by *in situ* formation, varies. Furthermore, the location of IC deposition within the glomerulus and the subsequent complement activation can

determine the type of injury that occurs. The injurious or protective effect of certain complement components in the pathogenesis of proliferative IC–GN has been described in different complement-deficient mouse strains treated with lipopolysaccharide (LPS) and horse spleen apoferritin (HSA). These results showed that complement components C3 and C5, when induced locally, contributed to interstitial injury more than to glomerular lesions, while constitutively expressed local C4 was protective [12–14]. Kidney tissue is particularly vulnerable to complement-mediated damage due to the low expression of complement regulatory proteins on glomerular and tubular cells [15]. Complement regulatory protein Crry (complement receptor 1-related gene/protein y), a membrane-bound C3 convertase inhibitor, can protect from C3 deposition and renal impairment in different experimental models of nephritis [16]. In contrast to complement, the role that natural and inducible IgM plays in the pathophysiology of progressive IC–GN is not entirely clear. IgM, through its pentameric structure, can bind to several antigenic determinants per molecule, and due to its polyreactivity bind to several antigens simultaneously [2]. IgM pentamers can trigger the classical pathway of

complement activation which results directly in the activation of the central complement component C3, in the lysis of invading bacteria due to activation of the membrane attack complex (MAC) and in the opsonization of infectious particles for efficient phagocytosis by macrophages and polymorphonuclear leucocytes [3–5]. In addition, IgM can either bind LPS directly or on whole Gram-negative bacterial cells [17,18]. To extend our understanding of the role of IgM in IC–GN, we administered LPS and HSA to mice deficient in secretion of IgM but capable of expressing surface IgM and IgD and secreting other classes of immunoglobulins, and investigated glomerular and tubulo-interstitial tissue damage, local C3 synthesis, C3 deposition and apoptosis.

Materials and methods

Animals and experimental protocol

Mice deficient in secreted IgM (sIgM-deficient) on a mixed 129SvJ and C57BL/6 background were housed in specific pathogen-free facilities and experiments were performed according to institutional guidelines for animal use and care (GZ 66·009/74-Pr/4/2000, GZ 66·009/87-Pr/4/2002) [19]. IC–GN was induced in 8–12-week-old female sIgM-deficient ($n = 11$) and wild-type littermates ($n = 10$) with a body weight of 25–30 g by intraperitoneal injection of 0·05 mg LPS (from *Escherichia coli*, serotype O55:B5; Sigma, St Louis, MO, USA) three times a week and with 4 mg HSA (Sigma) five times a week for a total of 6 weeks [20]. At the end of the experiments, mice were housed in metabolic cages for 24 h for urine sample collection. Urine protein and creatinine levels were measured on an Olympus AU 5400 analyser (Olympus Diagnostica, Hamburg, Germany) and assessment of small molecular weight proteins in the urine was performed by sodium dodecyl sulphate-polyacrylamide gel electrophoresis (SDS-PAGE) [21].

Histological analysis, immunohistochemistry and confocal laser scanning microscopy

Renal tissue was fixed in paraformaldehyde and 4 µm paraffin sections were stained with haematoxylin and eosin (H&E), periodic acid Schiff (PAS), Masson's Trichrome and methinamine silver. Glomerular cellularity and glomerular size were assessed in areas of 20 equatorially sectioned glomeruli; the renal area and the number of glomeruli were counted in ten 1 mm² fields selected at random on PAS-stained paraffin sections. Morphometric analysis was performed by two investigators independently [22]. For immunohistochemistry and immunofluorescence, renal tissue was embedded in optimal cutting temperature (OCT) compound (Tissue-Tek, Tokyo, Japan), snap-frozen in liquid nitrogen and stored at −80°C. Acetone fixed tissue sections (4 µm) were incubated with biotinylated rat anti-mouse

C3 monoclonal antibody (mAb) (0·25 µg/ml; Connex, Martinsted, Germany), with biotinylated hamster anti-mouse FasL (1 µg/ml; Pharmingen, San Jose, CA, USA) and with fluorescein isothiocyanate (FITC)-conjugated alpha smooth muscle actin (αSMA, 1 µg/ml; Sigma) in Tris-buffered saline (TBS)/1% bovine serum albumin (BSA) overnight at 4°C. Binding of biotinylated antibodies was detected using peroxidase-conjugated streptavidin (extravidin POD, 20 µg/ml; Sigma) and the FITC antibody was detected using horseradish peroxidase (HRP)-conjugated anti-FITC antibody (1·5 U/ml; Roche, Penzberg, Germany). The sections were exposed to 3-amino-9-ethylcarbazole (AEC; Sigma) and counterstained with Mayer's haemalum. For two-colour immunohistochemistry renal tissue was incubated with a biotinylated rat anti-mouse C3 mAb (0·25 µg/ml; Connex), with FITC-conjugated rat anti-mouse CD11b mAb (1 µg/ml; Serotec, Oxford, UK), or alternatively with HRP-labelled peanut agglutinin (PNA, 8 µg/ml; Axell, Westbury, NY, USA) overnight at 4°C. Bound C3 mAb was detected by incubation with extravidin–alkaline phosphatase (AP, 3 µg/ml; Sigma) and by subsequent exposure to Fast Blue (Sigma), CD11b mAb by an HRP-conjugated anti-FITC antibody (1·5 U/ml; Roche) and AEC precipitation. Endogenous peroxidase was blocked by adding D-glucose and glucose oxidase type VII. To assess renal IgG, IgM and C3 IC deposits by immunofluorescence and confocal laser scanning microscopy, FITC-conjugated rat anti-mouse IgM (5 µg/ml; Pharmingen), purified goat anti-mouse C3 (4 µg/ml; Cappel, Aurora, CA, USA) and biotin-conjugated horse anti-mouse IgG (H + L) antibody (1 µg/ml; Vector, Burlingame, CA, USA) were diluted in TBS/1% BSA and applied overnight at 4°C. Detection was performed with tetra-methylrhodamine isothiocyanate (TRITC)-conjugated rabbit anti-goat IgG F(ab′)₂ (1·4 µg/ml; Jackson Immunoresearch, West Grove, PA, USA) and streptavidin Cy5-conjugate (2 µg/ml; Jackson Immunoresearch). Pro-apoptotic molecules were traced by incubation with purified rabbit anti-mouse active caspase 3 antibody (5 µg/ml; Pharmingen), followed by goat anti-rabbit Alexa Fluor 488 and phycoerythrin (PE)-conjugated hamster anti-mouse Fas (2 µg/ml; Pharmingen). Serial dilutions of each primary and secondary antibody were performed to minimize non-specific binding, to ensure separation of fluorescent signals and to optimize fluorophore concentration to preclude self-quenching. Sections were analysed with a confocal laser scanning microscope (LSM 510; Zeiss, Oberkochen, Germany) with multi-photon laser (argon laser: 488 nm for FITC and Alexa Fluor 488, HeNe1: 543 nm for TRITC and PE, HeNe2: 633 nm for Cy5) and a 63× Zeiss Plan–Apochromat differential interface contrast oil immersion objective.

Assessment of apoptotic DNA fragmentation

To detect apoptotic DNA fragmentation, frozen tissue sections were stained using the ApopTag *in situ* apoptosis

detection kit (Chemicon, Temecula, CA, USA) modified by the use of a biotin-conjugated anti-digoxigenin antibody (1:1000; Sigma), extravidin AP-conjugate (1:400; Sigma) and subsequent exposure to Fast Blue (Sigma). The total number of apoptotic cells per renal cross-section was assessed by morphometric analysis and displayed as apoptotic cells/mm^2.

Reverse transcription–polymerase chain reaction (RT–PCR) and fluorogenic real-time RT–PCR

Total RNA was isolated from snap-frozen renal tissue samples using the TRIzol reagent (Life Technologies, Gaithersburg, MD, USA) and contaminating DNA was removed by DNase I treatment using a DNA-free kit (Ambion, Austin, TX, USA) as described previously [23]. Total RNA was quantified by spectrophotometry at 260 nm and equal amounts (3 μg) of total RNA were used for first-strand cDNA synthesis (SuperScript first-strand synthesis system; Invitrogen, Carlsbad, CA, USA). Equal amounts of cDNA were amplified in a gradient thermocycler (Hybaid, PCR Express, Ashford, UK) employing *Taq* DNA polymerase (Life Technologies) and oligonucleotide primer pairs specific for murine hypoxanthine-quanine phosphoribosyltransferase (HPRT) (sense 5′-CACAGGACTAGAACAACCTGC-3′ and anti-sense 5′-GCTGGTGAAAAGGACCTCT-3′; product length 249 kb) and murine C3 (sense 5′-GGCTGACTCTGTGTGGGT-3′ and anti-sense 5′-GCACGTGGTCTCTTCTGT-3′; product length 706 kb). The PCR amplification profile involved 35 cycles of denaturation at 94°C for 20 s, primer annealing at primer-specific temperatures (59°C for HPRT; 58°C for C3) for 30 s and primer extension at 72°C for 45 s, with a final extension step at 72°C for 10 min. Ten μl PCR-generated products were resolved by electrophoresis on 2% agarose gels, exposed to ultraviolet light using the EpiChemi II Darkroom (UVP, Upland, CA, USA) and photographed with a Camedia C-3040 digital camera (Olympus, Tokyo, Japan). For fluorogenic real-time RT–PCR the concentration of cDNA of all samples was determined with the OliGreen ssDNA quantification kit (Molecular Probes, Eugene, OR, USA), equal amounts (16 ng) of cDNA were amplified in an ABI Prism 7700 sequence detection system (Applied Biosystems, Foster City, CA, USA) using the Platinum Quantitative SuperMix-UDG (Invitrogen) and oligonucleotide LUX primer pairs specific for murine glyceraldehyde-3-phosphate dehydrogenase (GAPDH) (6-carboxy-4′,5′dichloro-2′,7′ dimethoxy-fluorescein [JOE]-labelled sense 5′-CACCAT CCCTGCATCCACTGG6G-3′, anti-sense 5′-CCAGTGAG CTTCCCGTTCAG-3′) and for murine C3 (6-carboxy fluorescein [FAM]-labelled sense 5′-GAACTTAGGGCAACGC AAG5TC-3′; anti-sense 5′-TCGAGCTTCAGGGCGTTTC-3′). The amplification protocol employed incubation at 50°C for 2 min, 95°C for 2 min and 40 cycles of denaturation at 95°C for 15 s, annealing at 55°C for 30 s and extension at 72°C for 15 s. The threshold was set at a fluorescence intensity of 0·03. Fluorescence was monitored during every PCR cycle at the annealing and extension steps. Efficiency-corrected relative quantification was performed by the 2$^{-\Delta\Delta CT}$ method.

Statistical analysis

Differences in glomerular cellularity and number of apoptotic cells detected by morphometric analysis between sIgM-deficient and wild-type mice were calculated using the Mann–Whitney *U*-test (SPSS GmbH Software, Munich, Germany). Results are shown as mean ± standard deviation (s.d.). Quantitative PCR data were compared by non-parametric analysis using the Mann–Whitney *U*-test; *P*-values < 0·05 were considered statistically significant.

Results

Bound C3 is shifted from the glomerulus to the tubulo-interstitial compartment in LPS/HSA-treated sIgM-deficient mice

To develop an IC–GN, sIgM-deficient and wild-type littermates were injected intraperitoneally with 0·05 mg LPS three times a week and 4 mg HSA five times weekly for a total of 6 weeks, and early signs of mesangial and endocapillary proliferation were detected by histochemical analysis (Fig. 1). The size of glomeruli (LPS/HSA-treated sIgM-deficient mice 1·69 ± 0·11 mm^2, LPS/HSA-treated wild-type mice 1·79 ± 0·18 mm^2), the number of glomeruli per renal cross-section (LPS/HSA-treated sIgM-deficient mice 240 ± 36 glomeruli, LPS/HSA-treated wild-type mice 211 ± 83 glomeruli) and glomerular cellularity (LPS/HSA-treated sIgM-deficient mice 59·3 ± 4·2 cells/glomerular cross-section (gcs); LPS/HSA-treated wild-type mice 58·4 ± 5·9 cells/gcs) after 6 weeks was equivalent in both treated groups as determined by morphometric analysis and did not differ from the untreated groups (glomerular size: sIgM-deficient mice 1·29 ± 0·16 mm^2; wild-type mice 1·45 ± 0·15 mm^2; number of glomeruli per cross-section: sIgM-deficient mice 177 ± 26; wild-type mice 151 ± 18, glomerular cellularity: sIgM-deficient mice 52·7 ± 1·9 cells/gcs; wild-type mice 61·8 ± 5·4 cells/gcs). Immunohistochemistry assessing the distribution of C3 protein revealed distinct staining patterns in sIgM-deficient and wild-type mice (Fig. 2a–f). Whereas strong mesangial and weak tubulo-interstitial C3 staining was found in LPS/HSA-treated wild-type mice (Figs 2a,c,e and 3a,b), LPS/HSA-treated sIgM-deficient mice showed, in addition to mesangial C3 deposits, strong staining of Bowman's capsule and tubular basement membrane (Figs 2b,d,f and 3e,f). Double-immunolabelling with mC3 mAb and PNA, a lectin that binds to structures in the lumen of distal tubules, showed that C3 bound preferentially to the basement membrane of proximal tubules in LPS/HSA-treated sIgM-deficient mice (Fig. 2d). In contrast, unmanipulated mice of

Wild-type   slgM⁻/⁻
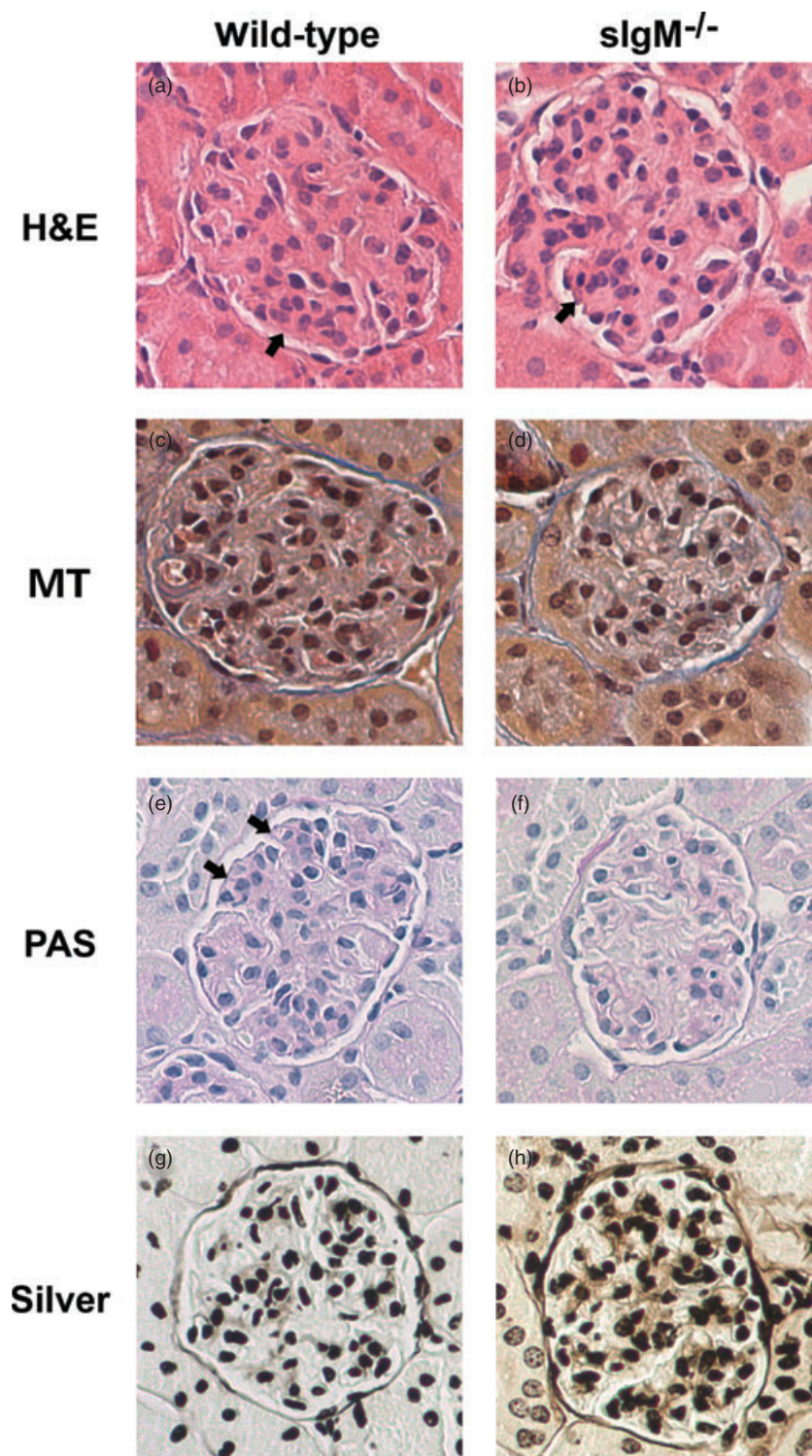
Fig. 1. Histochemical analysis of kidney sections from lipopolysaccharide/horse spleen apoferritin (LPS/HSA)-treated sIgM-deficient and wild-type animals. Secreted IgM (sIgM)-deficient and wild-type mice were treated with intraperitoneal injection of 0·05 mg LPS three times a week and 4 mg HSA five times a week. After 6 weeks renal tissue was fixed in paraformaldehyde and 4 μm paraffin sections were stained with haematoxylin and eosin (H&E), Masson's Trichrome (MT), periodic acid Schiff (PAS) and methinamine silver (Silver) according to standard protocols. Ongoing mesangial and endocapillary hypercellularity occurs in both experimental groups alike and is indicated by arrows. Magnification × 250.

either genotype showed faint tubular C3 staining, and slight discontinuous C3 staining of the Bowman's capsule (data not shown) [24]. An insignificant increase of infiltrating CD11b+ macrophages was found in LPS/HSA-treated sIgM-deficient mice (68·5 ± 25·09 CD11b+ macrophages/mm²) compared to LPS/HSA-treated wild-type mice (43·96 ± 13·01 CD11b+ macrophages/mm²). No difference in the number of CD11b+ macrophages located within the glomerular area was observed in the two LPS/HSA-treated experimental groups (sIgM-deficient mice 35·31 ± 14·77 CD11b+ macrophages/
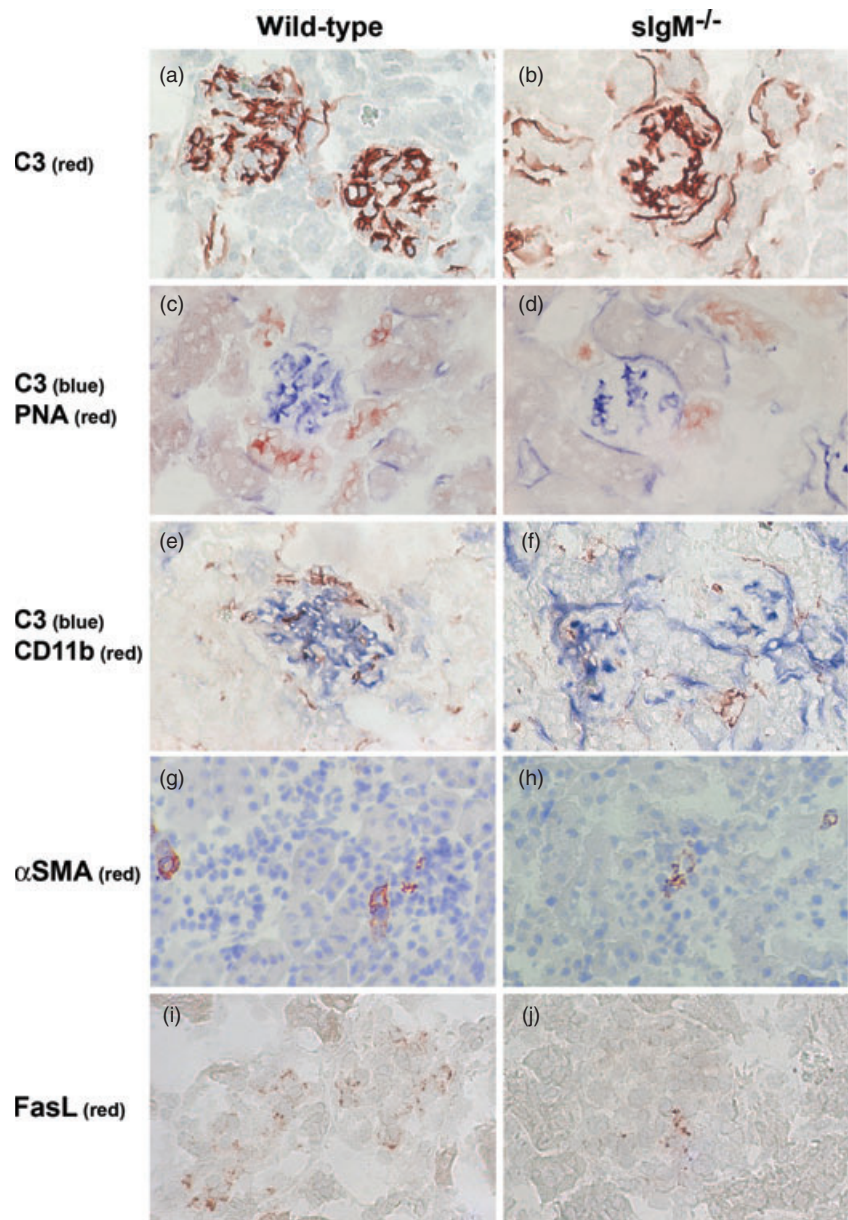
Fig. 2. Immunohistochemical determination of C3 deposits on proximal tubules and CD11b expression on macrophages in kidney sections of lipopolysaccharide/horse spleen apoferritin (LPS/HSA)-treated secreted IgM (sIgM)-deficient and wild-type littermates. Only mesangial deposits of C3 (red) were found in treated wild-type mice (a), while C3 also bound to the Bowman's capsule and to proximal tubules in treated sIgM-deficient mice (b). C3 (blue) does not bind to distal tubules of LPS/HSA-treated sIgM-deficient (d) and wild-type mice (c) stained with PNA (red). Infiltrating CD11b+ macrophages (red) were found scattered intra- and periglomerular in LPS/HSA-treated wild-type mice (e) and more in the interstitial compartment in LPS/HSA-treated sIgM-deficient (f); sections were counterstained with C3 (blue). No signs of myofibroblast transformation indicated by alpha smooth muscle actin binding was observed (g, h). Glomerular FasL (red) expression was found to be stronger in LPS/HSA-treated wild-type mice (i) than in treated sIgM-deficient mice (j). Magnification × 250.

mm^2, wild-type mice 26·72 ± 10·29 CD11b+ macrophages/mm^2), while more infiltrating CD11b+ macrophages were found in the periglomerular area of LPS/HSA-treated sIgM-deficient mice (sIgM-deficient mice 30·66 ± 12·39 CD11b+ macrophages/mm^2, wild-type mice 17·24 ± 4·96 CD11b+ macrophages/mm^2) (Fig. 2e,f). No signs of interstitial fibrosis due to myofibroblast transition identified by αSMA staining could be found in LPS/HSA-treated sIgM-deficient or wild-type mice; αSMA was detected exclusively on pericytes in vessel walls (Fig. 2g,h). Co-localization studies of C3, IgM and IgG by confocal laser scanning microscopy supported the observations found by immunohistochemistry. A granular mesangial staining pattern for C3 and faint staining of the Bowman's capsule and the tubular basement membrane was found in LPS/HSA-treated wild-type mice (Fig. 3a,b) that co-localized with IgM and IgG staining (Fig. 3a–d). Interestingly, fluorescence intensity appeared to be higher for IgM than for IgG. In LPS/HSA-treated sIgM-deficient mice, C3 was located along the Bowman's capsule and the tubular basement membrane with only focal mesangial staining (Fig. 3e,f,h). Trace diffuse mesangial IgG staining, but no tubular deposits of IgG were found in the absence of IgM (Fig. 3d,h).

Increased levels of low molecular weight protein in LPS/HSA-treated sIgM-deficient mice

Biochemical analysis of 24-h urine samples collected at the end of the experiment revealed an increase in protein (sIgM-deficient mice: 0·85 g/l, wild-type mice: 1·19 g/l) and creati-
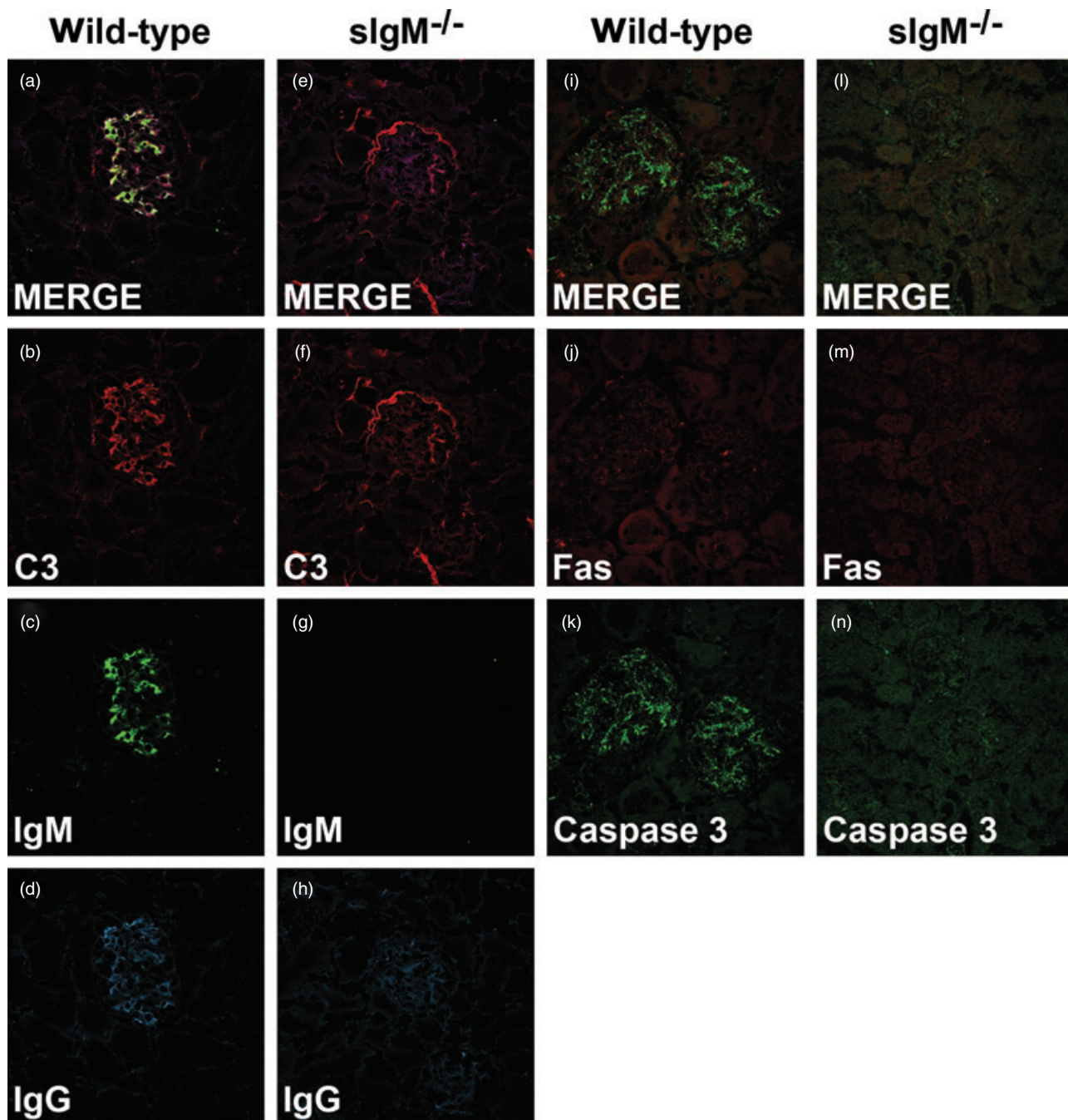
Fig. 3. Deposition of C3, IgM and IgG in renal tissue of lipopolysaccharide/horse spleen apoferritin (LPS/HSA)-treated sIgM-deficient and wild-type littermates detected by confocal laser scanning microscopy. Mesangial deposits of C3 (red), IgM (green) and IgG (blue) were found in treated wild-type mice (a–d). C3 (red) was found along the basement membrane of tubules and Bowman's capsule (e, f) with little mesangial staining in treated secreted IgM (sIgM)-deficient mice, while trace amounts of IgG (blue) could be observed on the mesangium (h). Strong caspase 3 (i, k) and only trace Fas (i, j) expression in glomeruli of treated wild-type mice, while no caspase 3 (l, n) or Fas (l, m) could be found in glomeruli of treated sIgM-deficient mice. Magnification × 630.

nine (sIgM-deficient mice: 44·0 mg/dl, wild-type mice: 38·5 mg/dl) in LPS/HSA-treated sIgM-deficient and wild-type mice compared to untreated controls (protein < 0·1 g/l, creatinine < 25·0 mg/dl). Assessment of urinary proteins by SDS-PAGE in 24-h urine samples resulted in detection of a 30-kDa low molecular weight protein in LPS/HSA-treated sIgM-deficient mice only (Fig. 4a), reflecting dysfunction of the proximal renal tubules [25,26].

(a)

(b)
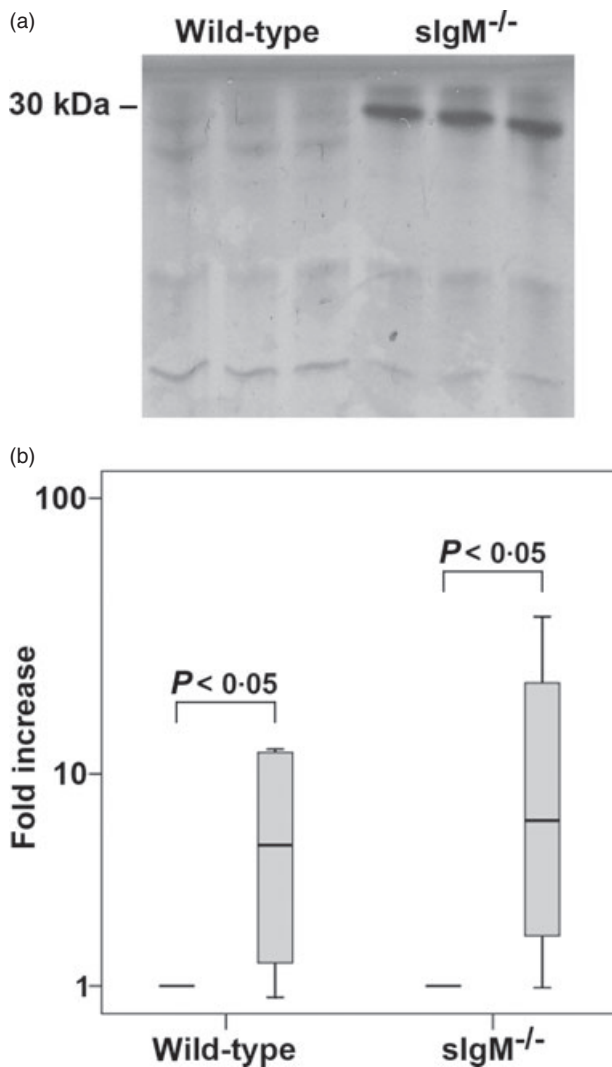
Fig. 4. (a) Sodium dodecyl sulphate-polyacrylamide gel electrophoresis of 24-h urine samples of secreted IgM (sIgM)-deficient and wild-type animals after 6 weeks of lipopolysaccharide/horse spleen apoferritin (LPS/HSA) treatment. A 30 kDa low molecular weight protein was found in urine samples of LPS/HSA-treated sIgM-deficient mice (lanes 4, 5, 6), but not in the urine of wild-type animals (lanes 1, 2, 3). (b) Quantitative fluorogenic reverse transcription–polymerase chain reaction of mC3. C3 expression is increased significantly in LPS/HSA treated animals (box plots) compared to untreated animals of each experimental group. C3 expression was calculated by the $2^{-\Delta\Delta CT}$-method normalized to the highly expressed housekeeping gene glyceraldehyde-3-phosphate dehydrogenase, relative to C3 expression of untreated animals of the corresponding genotype. Significant increase of C3 expression was found between untreated and treated animals, whereas no statistically significant difference in C3 expression could be detected between both LPS/HAS-treated groups. Statistical significance P is based on the Mann–Whitney U-test.

Comparable levels of C3 mRNA in kidney tissue of LPS/HSA-treated sIgM-deficient and wild-type littermates

When C3-specific RT–PCR was performed with cDNA generated from equal amounts of total RNA obtained from kidney tissue of LPS/HSA-treated sIgM deficient and wild-type mice, no difference was found in the amount of C3 mRNA (data not shown). To apply a more sensitive method, fluorogenic quantitative real-time PCR was chosen to assess C3 mRNA levels (Fig. 4b). C3 expression was calculated by the $2^{-\Delta\Delta CT}$ method nomalized to the highly expressed housekeeping gene GAPDH, relative to C3 expression of untreated animals of the corresponding genotype. Significant increase of C3 expression was found between untreated and LPS/HSA-treated mice (in sIgM-deficient mice a $19·5 \pm 8$ and in wild-type mice a $6·2 \pm 2$-fold increase normalized to GAPDH expression), whereas no statistical difference in C3 expression could be detected between both LPS/HSA-treated groups (Fig. 4b).

Apoptotic DNA fragmentation in glomerular cells and pro-apoptotic molecules

Visualization of nuclei of apoptotic cells by the Apoptag *in situ* apoptosis detection kit showed more apoptotic nuclei in LPS/HAS-treated wild-type animals compared to LPS/HSA-treated sIgM-deficient mice (sIgM-deficient mice $0·9 \pm 0·2$ apoptotic nuclei/mm^2, wild-type mice $3·1 \pm 1·1$ apoptotic nuclei/mm^2). When apoptotic cells were detected, they were found predominantly within the glomeruli and not in the tubulo-interstitial compartment. Accordingly, increased glomerular expression of FasL (Fig. 2i,j), Fas and caspase 3 (Fig. 3i–n) was found in LPS/HSA-treated wild-type mice by immunohistochemistry and immunofluorescence, compared to LPS/HSA-treated sIgM-deficient mice, and no sign of apoptosis was detected in renal tissue of untreated mice (data not shown).

Discussion

The role of IgM antibodies in the pathophysiology of IC–GN induced by repeated treatment with LPS and HSA for 6 weeks was investigated in mice deficient in the production of sIgM, but capable of expressing surface IgM and IgD and secreting other classes of immunoglobulins. The size of the glomeruli, the number of glomeruli per renal cross-section and glomerular cellularity in LPS/HSA-treated sIgM-deficient and wild-type mice did not differ statistically significantly from untreated mice, but urine analysis showed increased levels of protein and creatinine in both LPS/HSA-treated groups compared to untreated mice. In LPS/HSA-treated sIgM-deficient mice, C3 and IgG antibody could bind to the Bowman's capsule and tubular basement membrane

and to the mesangium. In LPS/HSA-treated wild-type mice, in contrast, C3 and IgM/IgG antibodies were found exceptionally on the mesangium. Interestingly, IgM has no effect on the glomerulus in this model of experimental IC–GN, where LPS can bind to natural IgM antibodies and where repeated treatment of mice with LPS/HSA induces specific IgM and IgG antibodies for LPS and HSA [17,18,24,27]. Immune deposits form when anti-LPS/HSA antibodies bind specifically to soluble LPS/HSA that become localized in the glomerulus and, dependent upon the position where ICs precipitate, they can disrupt the glomerular architecture by activating the complement pathway and recruit leucocytes. Complement present within the ICs can function as a mediator linking antibody deposition with glomerular dysfunction and tissue injury, but can also influence glomerular handling of IC by changing its physiochemical characteristics [28,29]. Previous work using LPS/HSA-treated complement C3-, C4- and C5-deficient mice showed no apparent difference in glomerular injury when compared to wild-type mice, but a mechanism was described as to how a primary glomerular process could progress to involve the tubulo-interstitial compartment in a complement-dependent manner [12–14,30,31]. In the initial phase of GN, the complement source is the circulation as the amount of complement mRNA detected in healthy kidney, with the exception of C4, is low. During the course of glomerular injury a variety of cytokines are expressed by mesangial cells or infiltrating leucocytes to induce complement production locally within the glomeruli [32]. Cytokines can also gain access to the epithelium of the Bowman's capsule and to the proximal tubular epithelium via the glomerular filtrate, inducing local complement production within the tubulo-interstitial compartment [32]. Furthermore, complement-dependent damage to glomerular, tubular or interstitial cells can cause exposure of previously hidden cell membrane antigens and binding of 'natural antibodies', predominantly of the strongly complement-activating IgM isotype, leading to additional propagation of the classical complement pathway [4,5]. It has already been shown that this translocation of local C3 production from the glomeruli into kidney interstitium has a serious impact on disease outcome of progressive IC–GN [29,30]. Once C3 is present in the interstitium, the ammonia content of the interstitium can result in the formation of $NH_3 \cdot C3$, an effective convertase; during cell injury, proximal tubular epithelial cells become alternative pathway activators [14,31,33]. Experiments on sIgM-deficient mice helped to identify the specific role of IgM antibodies in this complex scenario. LPS/HSA-treated sIgM-deficient mice in our model showed strong C3 staining of the basement membrane of proximal tubules and interstitial CD11b+ macrophages, and in the urine a 30 kDa low molecular weight protein was found, reflecting chronic dysfunction of the proximal renal tubuli. In contrast, LPS/HSA-treated wild-type mice showed less interstitial C3 staining, although whole kidney C3 mRNA quantified by real-time RT–PCR was comparable between the two experimental groups. Furthermore, fewer CD11b+ macrophages were found in the tubulo-interstitial compartment of LPS/HSA-treated wild-type mice, and no low molecular weight protein appeared in the urine. These infiltrating CD11b+ macrophages can bind C3 fragment C3bi, leading to further C3 production by activated macrophages [14,34].

Cell death by apoptosis is an essential physiological process for the maintenance of normal kidney homeostasis and for the safe clearance of damaged kidney cells during resolution of inflammation in the early stage of GN [35,36]. In our model of IC–GN, apoptosis, FasL, Fas and caspase 3 expression were found predominantly in glomerular cells of LPS/HSA-treated wild-type mice, but not in LPS/HSA-treated sIgM-deficient mice. The relatively few numbers of apoptotic cells found in LPS/HSA-treated wild-type mice did not affect glomerular cellularity. Interstitial cells and tubular cells of both LPS/HSA-treated groups showed no signs of apoptosis. These results indicate that sIgM is involved in the regulation of apoptosis in glomerular cells and glomerular infiltrating leucocytes, leading to efficient clearance by macrophages and mesangial cells. When IC–GN progresses further, tubulo-interstitial apoptosis, interstitial collagen deposition and myofibroblast transition identified by αSMA staining occur as signs of progressive fibrosis [29,32,35].

Our results indicate that sIgM can protect the tubulo-interstitial compartment from LPS- and HSA-induced GN by preventing early translocation of C3 from the glomerulus to the tubulo-interstitial tissue, and can propagate apoptosis in order to maintain clearance. Although IgM is unlikely to be the sole mediator protecting from interstitial injury accompanying progressive disease, as C4, C1q, the C3 inhibitor sCR1 and IgG also have an effect, our study can help to show the complex and fine-tuned interplay between IgM antibodies and the complement system in the pathophysiology of IC–GN.

References

1 Fearon DT, Locksley RM. The instructive role of innate immunity in the acquired immune response. Science 1996; **272**:50–3.

2 Boes M. Role of natural and immune IgM antibodies in immune responses. Mol Immunol 2000; **37**:1141–9.

3 Ault BH, Colten HR. Cellular specificity of murine renal C3 expression in two models of inflammation. Immunology 1994; **81**:655–60.

4 Sheerin NS, Springall T, Abe K *et al.* Protection and injury: the differing roles of complement in the development of glomerular injury. Eur J Immunol 2001; **31**:1255–60.

5 Berger SP, Roos A, Daha MR. Complement and the kidney: what the nephrologist needs to know in 2006? Nephrol Dial Transplant 2005; **20**:2613–19.

6 Abe K, Miyazaki M, Koji T *et al.* Intraglomerular synthesis of complement C3 and its activation products in IgA nephropathy. Nephron 2001; **87**:231–9.

7 Anders HJ, Vielhauer V, Kretzler M *et al.* Chemokine and chemokine receptor expression during initiation and resolution of immune complex glomerulonephritis. J Am Soc Nephrol 2001; **12**:919–31.

8 Montinaro V, Lopez A, Monno R *et al.* Renal C3 synthesis in idiopathic membranous nephropathy: correlation to urinary C5b-9 excretion. Kidney Int 2000; **57**:137–46.

9 Brown KM, Kondeatis E, Vaughan RW *et al.* Influence of donor C3 allotype on late renal-transplantation outcome. N Engl J Med 2006; **354**:2014–23.

10 Pratt JR, Basheer SA, Sacks SH. Local synthesis of complement component C3 regulates acute renal transplant rejection. Nat Med 2002; **8**:582–7.

11 Pratt JR, Abe K, Miyazaki M *et al. In situ* localization of C3 synthesis in experimental acute renal allograft rejection. Am J Pathol 2000; **157**:825–31.

12 Welch TR, Blystone LW. C3 is central to the interstitial complement of experimental immune complex glomerulonephritis. Clin Immunol 2005; **115**:80–4.

13 Welch TR, Frenzke M, Carroll MC *et al.* Evidence of a role for C4 in modulating interstitial inflammation in experimental glomerulonephritis. Clin Immunol 2001; **101**:366–70.

14 Welch TR, Frenzke M, Witte D *et al.* C5a is important in the tubulointerstitial component of experimental immune complex glomerulonephritis. Clin Exp Immunol 2002; **130**:43–8.

15 Kitamura M, Fine LG. The concept of glomerular self-defense. Kidney Int 1999; **55**:1639–71.

16 Quigg RJ, He C, Lim A *et al.* Transgenic mice overexpressing the complement inhibitor Crry as a soluble protein are protected from antibody-induced glomerular injury. J Exp Med 1998; **188**:1321–31.

17 Reid RR, Prodeus AP, Khan W *et al.* Endotoxin shock in antibody-deficient mice: unraveling the role of natural antibody and complement in the clearance of lipopolysaccharide. J Immunol 1997; **159**:970–5.

18 Proxton IR. Antibodies to lipopolysaccharide. J Immunol Methods 1995; **186**:1–15.

19 Boes M, Esau C, Fischer MB *et al.* Enhanced B-1 cell development, but impaired IgG antibody response in mice deficient in secretory IgM. J Immunol 1998; **160**:4776–87.

20 Welch TR, Frenzke M, Witte D. Evidence of a role for local complement expression in a murine model of progressive glomerulonephritis. Pediatr Res 2000; **48**:200–5.

21 Bazzi C, Petrini C, Rizza V *et al.* Characterization of proteinuria in primary glomerulonephritides. SDS-PAGE patterns: clinical significance and prognostic value of low molecular weight ('tubular') proteins. Am J Kidney Dis 1997; **29**:27–35.

22 Fischer MB, Goerg S, Shen L *et al.* Dependence of germinal center B cells on expression of CD21/CD35 for survival. Science 1998; **280**:582–5.

23 Rüger B, Giurea A, Wanivenhaus AH *et al.* Endothelial precursor cells in the synovial tissue of patients with rheumatoid arthritis and osteoarthritis. Arthritis Rheum 2004; **50**:2157–66.

24 Quigg RJ, Lim A, Haas M *et al.* Immune complex glomerulonephritis in C4- and C3-deficient mice. Kidney Int 1998; **53**:320–30.

25 Leheste JR, Rolinski B, Vorum H *et al.* Megalin knockout mice as an animal model of low molecular weight proteinuria. Am J Pathol 1999; **155**:1361–70.

26 D'Amico G, Bazzi C. Pathophysiology of proteinuria. Kidney Int 2003; **63**:809–25.

27 Li M, O'Sullivan KM, Jones LK *et al.* CD100 enhances dendritic cell and CD4+ cell activation leading to pathogenetic humoral response and immune complex glomerulonephritis. J Immunol 2006; **177**:3406–12.

28 Fujigaki Y, Nagase M, Kojima K *et al.* Glomerular handling of immune complex in acute phase of active *in situ* immune complex glomerulonephritis employing cationized ferritin in rats. Virchows Arch 1997; **431**:53–61.

29 Nangaku M, Couser WG. Mechanisms of immune-deposit formation and the mediation of immune renal injury. Clin Exp Nephrol 2005; **9**:183–91.

30 Sheerin NS, Sacks SH. Leaked protein and interstitial damage in the kidney: is complement the missing link? Clin Exp Immunol 2002; **130**:1–3.

31 Biancone L, David S, Della Pietra V *et al.* Alternative pathway activation of complement by cultured human proximal tubular epithelial cells. Kidney Int 1994; **45**:451–60.

32 Camussi G, Ronco C, Montruchio G *et al.* Role of soluble mediators in sepsis and renal failure. Kidney Int 1998; **53**:38–42.

33 Nath KA, Hostetter MK, Hostetter TH. Pathophysiology of chronic tubulo-interstitial disease in rats. Interactions of dietary acid load, ammonia, and complement C3. J Clin Invest 1985; **76**:667–75.

34 Tang T, Rosenkranz A, Assmann KJ *et al.* A role for Mac-1 (CDIIb/CD18) in immune complex-stimulated neutrophil function *in vivo*: Mac-1 deficiency abrogates sustained Fcgamma receptor-dependent neutrophil adhesion and complement-dependent proteinuria in acute glomerulonephritis. J Exp Med 1997; **186**:1853–63.

35 Ortiz A, Gonzales CS, Lorz C *et al.* Apoptosis in renal diseases. Front Biosci 1996; **1**:30–40.

36 Taylor PR, Carugati A, Fadok VA *et al.* A hierarchical role for classical pathway complement proteins in the clearance of apoptotic cells *in vivo*. J Exp Med 2000; **192**:359–66.